Rafał Piotuch, Ryszard Pałka, Kamil Tarenko
West Pomeranian University of Technology Szczecin
Department of Power Systems and Electrical Drives

MASZYNA SYNCHRONICZNA MAŁEJ MOCY Z WIRNIKIEM PROSZKOWYM, WZBUDZANA MAGNESAMI TRWAŁYMI – WYNIKI BADAŃ SYMULACYJNYCH I EKSPERYMENTALNYCH

SMALL POWER SYNCHRONOUS MACHINE WITH SMC PM EXCITED ROTOR – EXPERIMENTAL AND SIMULATION RESULTS

Abstract: The work presented in this paper relates to an Interior Permanent Magnet Synchronous Motor (*IPMSM*) experimental and simulation results. The stator of the machine is an mass-produced one with classic assembly. The rotor has been previously optimized, designed and constructed and made of Soft Magnetic Composites (SMC). There is presented a method of measuring inductances at different load currents. Particularly self and mutual winding inductances as well as *d* and *q* axis inductances were evaluated. The value of torque was evaluated for different currents and power angles. Experimental results were compared with simulation ones. On the test stand there was also evaluated efficiency map.

Streszczenie: Artykuł przedstawia wyniki badań symulacyjnych i eksperymentalnych maszyny synchronicznej z magnesami zagnieżdżonymi. Stojan i korpus maszyny zostały zapożyczone z klasycznej maszyny asynchronicznej klatkowej. W trakcie wcześniejszych prac geometria wirnika została zoptymalizowana, zaprojektowana i wykonana w technologii proszków magnetycznych. Przedstawiono szczegóły metody użytej do wyznaczania indukcyjności dla różnych wartości prądu. W trakcie badań wyznaczono indukcyjności własne i wzajemne uzwojeń fazowych oraz w osi *d* i *q*. Pomierzono również wartości momentu obrotowego dla różnych wartości prądu w funkcji kąta mocy. Wyniki badań eksperymentalnych porównano z wynikami badań symulacyjnych. Na stanowisku pomiarowym wyznaczono również mapę sprawności badanej maszyny.

Keywords: PM electrical machines***, d, q inductances***
Słowa kluczowe: *maszyny wzbudzane magnesami trwałymi, indukcyjności d, q*

1. Introduction

To protect the environment, there exists a strong demand to develop very efficient electric motors with high torque/mass ratio [1-3]. Special design with high overall performance and wide speed operation capabilities [3, 4] make particular machines suitable for all automotive applications where weight and geometry dimensions are very important. An IPMSM with permanent magnets buried inside the rotor that is properly designed, fulfill foregoing requirements.

Main positive feature of SMC applied in magnetic cores is that it can be easily shaped in complex forms. The other advantage is its isotropic properties and low losses at high speed/frequencies. SMC mixed with epoxy resin makes machine structure robust to mechanical stresses. With proper technology it is possible to achieve high relative permeability up to 1000.

2. Machine geometry

The case of study is represented by a 4-pole IPMSM with fixed stator geometry and winding parameters. Stator and assembly are mass-produced ones taken from an induction motor. The machine is equipped with NdFeB magnets, oriented in the radial direction, mounted inside the rotor. Such structures are referred as IPM machines [3, 5]. The rotor is made of SMC (relative permeability approximately 40). During initial works there have been implemented optimization procedure in Matlab environment which used a genetic algorithm that ran and evaluated FE models in Maxwell tool [2, 5]. After optimization process the machine has been built and tested.

The analyzed geometry (optimized one without SMC poles) has been depicted in Fig. 1. and Fig. 2.

Selected machine parameters has been presented in the table 1.

Fig. 1. Initial rotor geometry (without iron poles) consecutive design stages

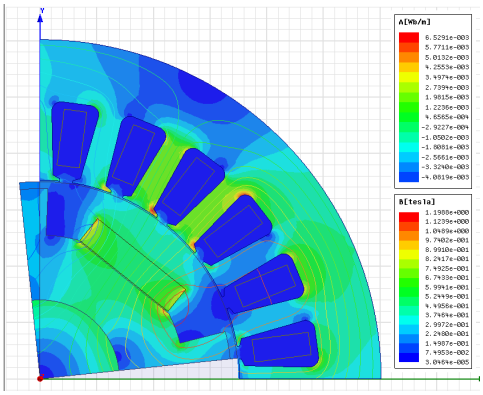

Fig. 2. Initial rotor geometry cross section

Tab. 1. Selected machine parameters

Parameter	Value	Unit
P_n	935	W
T_n	3.1	Nm
n_n	3000	rpm
H	88	%
I_n	1.6	A
R_s (20°C)	12.7	Ω
L_d	0.065	H
L_q	0.150	H

where:

P_n – nominal power

T_n – electromagnetic torque nominal value

n_n – nominal rounds per minute value

η – efficiency

I_n – nominal current

R_s – stator phase winding resistance

L_d, L_q – *d* and *q* axis inductances

p_b – number of pole pairs

m – machine mass

3. Simulation results

Simulations were conducted with a 2D FE model that did not consider any losses which caused some errors but on the other hand shorted calculation time. Characteristics of steel were taken from datasheet and were modeled as a nonlinear B-H curve. Magnet parameters were as follows (B_r=1.23T, H_c=-890kA/m). Fig. 3. shows torque waveforms as a function of power angle for two different current amplitude values. Electromagnetic torque consists of two main components according to (1):

$$T_{em} = \frac{3}{2} \cdot p_b \cdot \Psi_{PM} \cdot I_q + \frac{3}{2} \cdot p_b \cdot \left(L_d - L_q\right) \cdot I_d \cdot I_q \quad (1)$$

Where: I_d, I_q – *d* and *q* axis currents, Ψ_{PM} - magnet flux. The first one is a PM torque (that is proportional to quadrature axis current and flux in air gap developed by magnets), and the second one is a reluctance torque (that is proportional to the difference between direct and quadrature axis inductance, and currents product). The value of torque for nominal current and optimal power angle was about 3.1 Nm which is comparable with basic (induction motor) design (3.6 Nm).

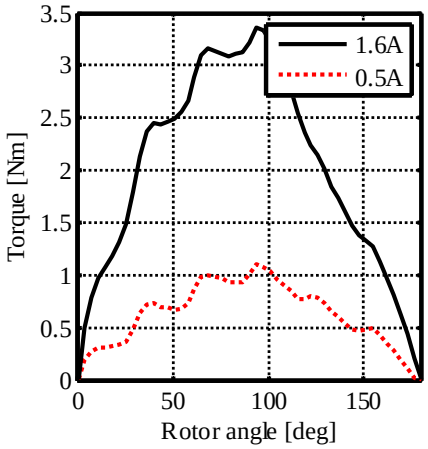

Fig. 3. Torque waveforms for different currents

Secondly L_A and L_{AB} values over different rotor position has been estimed using that method described in details in [6]. It must be emphasized that inductance values should be increased with end-winding inductances that has not been simulated in 2D model [7]. Recalculated results are shown in Fig. 4.

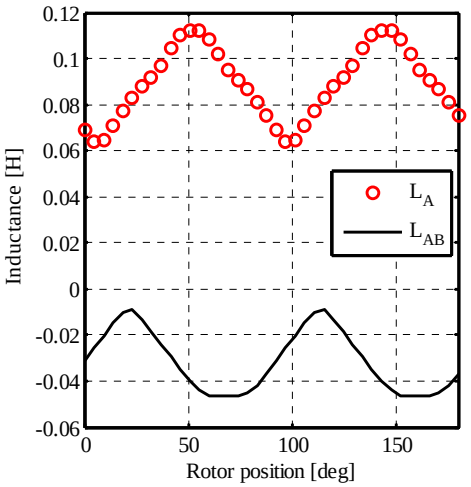

Fig. 4. Self and mutual inductance waveforms

L_d and L_q were 65mH and 150mH respectively. A method for calculation of *d* and *q* axis inductances values was described in [6]. Despite big magnet volume the PM flux value was relatively low - 400mWb.

Knowing machine parameters and power supply constraints it is possible to evaluate Constant Power Speed Range (CPSR). It has been defined as:

$$CPSR = \frac{\omega_{max}|_{P_n}}{\omega_n|_{P_n}} \tag{2a}$$

Theoretical considerations showed that proposed geometry has small CPSR (1.3), because it does not fulfill optimal field weakening condition:

$$I_n = \left| \frac{\Psi_{PM}}{L_d} \right| \tag{2b}$$

Torque and power curves are depicted in Fig. 5.

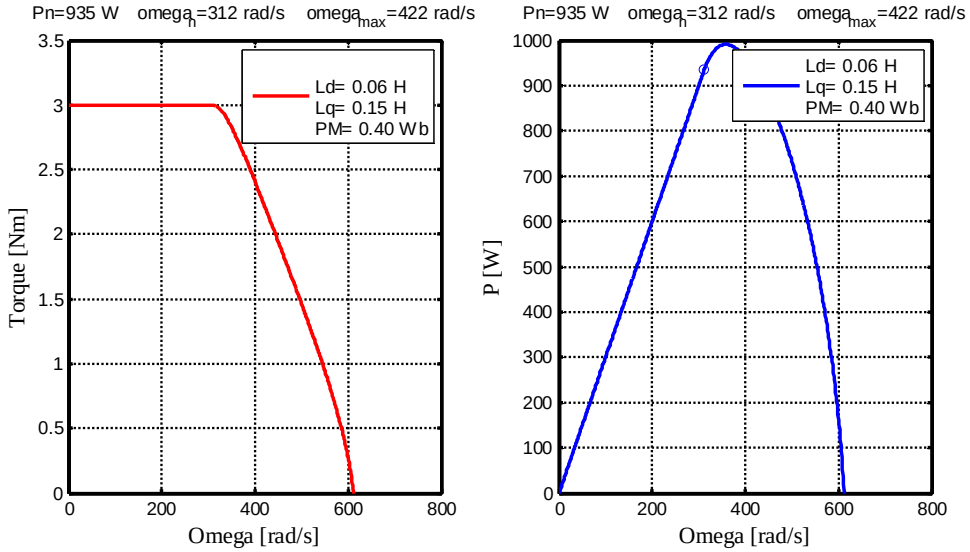

Fig. 5. Torque and power curves

Nominal speed of a proposed geometry was higher than for induction motor. For this reason it was possible to stay at even higher power level with smaller torque value.

4. Experimental results

For experimental evaluation of the machine parameters and characteristics, a proper test stand has been designed and programed (Fig. 6). It consists of the optimized IPM prototype and a B&R servo motor (8LSA44 - 1451W, 3000rpm) clutched and mounted on a aluminum plate, and several measurement devices. The B&R was controlled via application developed for Power Panel 45.

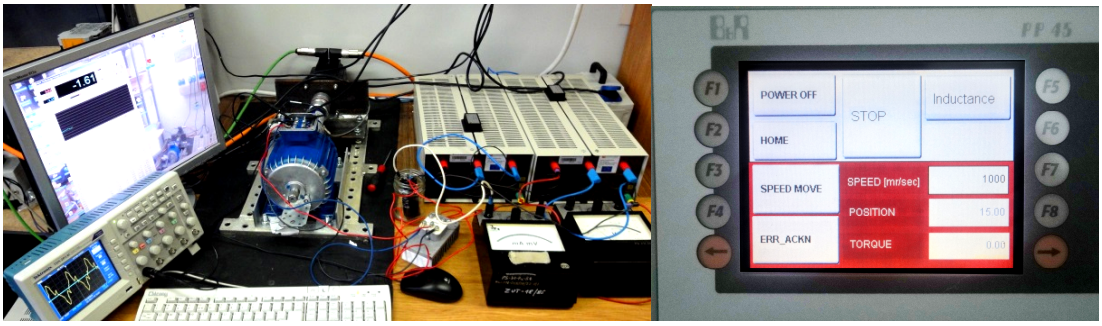

Fig. 6. Test stand

Inductance were measured with the scheme shown in Fig. 7.

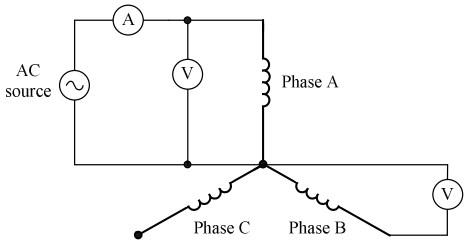

Fig. 7. Inductance measurement scheme

The inductances values were measured and calculated for 30 different positions with a 3deg step with the following formulas:

$$L_A(\varphi) = \frac{\sqrt{\left(\frac{U_A}{I_A}\right)^2 - R^2}}{2\pi f} \tag{3a}$$

$$L_{AB}(\varphi) = \frac{U_B}{(2\pi f) I_A} \tag{3b}$$

where

U_A, U_B – A and B phase RMS voltage value

L_A, L_{AB} – self and mutual inductance

f – AC source frequency

Fig. 8. shows self and mutual inductances values for different rotor positions and two AC currents – nominal and 1.5 times nominal value. It occurred that the machine was not saturated – for different currents there was nearly any change in the inductance values. It was caused by the relatively big air-gap length and low permeability of SMC.

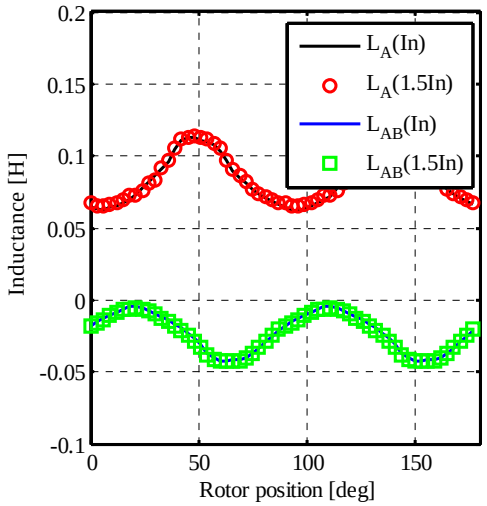

Fig. 8. Self and mutual inductance values

The machine efficiency was measured in generator regime for different speeds and load torques.

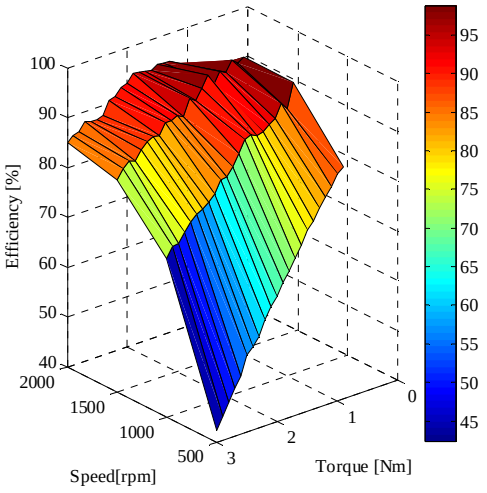

Fig. 9. Efficiency map

According to results shown in Fig. 10 the highest efficiency was about 96%.

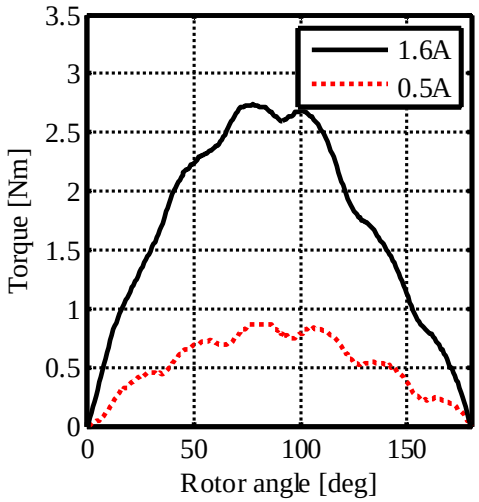

Fig. 10. Torque waveforms comparison

The last result show comparison of cogging torque waveforms (Fig. 12.). Experimental data needed some mathematical transformations, because torque level was very small and noise signal had a strong impact on a measured signal. Maximum value of cogging torque was about 2% of a nominal value so it was at acceptable level.

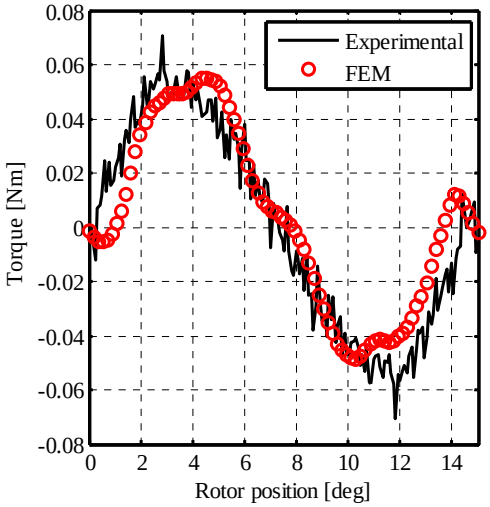

Fig. 11. Cogging torque waveforms comparison

5. Summary

Simulation results were validated experimentally. The prototype offered very high nominal efficiency (about 88% in contrary to induction motor efficiency – 73%) with very small maximum cogging torque value (about 0.05Nm – 2% of nominal value).

All these features were achieved due to PM excitation and rotor made of SMC. Negligible influence of current on d and q axis inductances values have been observed. It was caused by low permeability of SMC and high air gap length. Serious disadvantage of such solutions is small value of L_d, which results in limited field-weakening capabilities. During experimental evaluation it was not easy to keep constant temperature of windings – the copper wires were overheated in the high torque regions. Whole measurement procedure took about 8h for a qualified engineer. In the future there is planned a special test stand development that would simplify and automatize measurement procedures.

6. Literature

[1]. Paplicki P. The new generation of electrical machines applied in hybrid drive car, Electrical Review, Vol. 86, No. 6, 2010, 101-103.
[2]. Caramia R., Piotuch R., Pałka R., Multiobjective FEM based optimization of BLDC motor using Matlab and Maxwell scripting capabilities, Archives of Electrical Engineering, vol. 63(1), 2014, pp. 115-124.
[3]. Stumberger B., Hamler M., Trlep M., Jesenik M. Analysis of Interior Permanent Magnet Synchronous Motor Designed for Flux Weakening Operation, IEEE Transaction on Magnetics, Vol. 37, No. 5, 2001, pp. 3644-3647.
[4]. Paplicki P., Piotuch R., Improved Control System of PM Machine with Extended Field Control Capability for EV Drive, Mechatronics-Ideas for Industrial Application, Springer, part. I, Vol. 317, 2015, pp. 125-132.
[5]. Pałka R., Piotuch R., FEM based IPMSM optimization, Problem Issues - Electrical Machines, Vol. 104, No. 4, 2014, pp. 99-104.
[6]. Piotuch R. Inductance calculation considering magnetic saturation of interior permanent magnet synchronous machines, Informatyka, Automatyka Pomiary w Gospodarce i Ochronie Środowiska Vol. 2, 2013, pp. 29-33.
[7]. Zarko D., Ban D., Klari R. Finite Element Approach to Calculation of Parameters of an Interior Permanent Magnet Motor, AUTOMATIKA Vol. 46 No. 3-4, 2006, pp. 113–122

Authors

M.A. Rafał Piotuch, rafal.piotuch@zut.edu.pl
Prof. Ryszard Pałka, rpalka@zut.edu.pl
Kamil Tarenko, tk27274@zut.edu.pl student ,
West Pomeranian University of Technology Szczecin,
Department of Power Systems and Electrical Drives,
ul. Sikorskiego 37, 70-313 Szczecin,
tel.: +48 91 449 48 73